Available online at www.sciencedirect.com
ScienceDirect
Journal of Sound and Vibration 313 (2008) 7–15
JOURNAL OF SOUND AND VIBRATION
www.elsevier.com/locate/jsvi

Rapid Communication

Study on the two-phase critical flow through a small bottom break in a pressurized horizontal pipe

Moon-Sun Chung

Hydrogen Energy R & D Center, Korea Institute of Energy Research, 71-2 Jang-dong, Yuseong-gu, Daejeon 305-343, Republic of Korea

Received 8 January 2007; received in revised form 28 December 2007; accepted 14 January 2008
Handling Editor: J. Lam
Available online 6 March 2008

Abstract

Two-phase critical flow rates through a small bottom break of a pressurized horizontal pipe are calculated by using an improved critical flow model with a well-known quality prediction model. This phenomenon has many difficulties in predicting the two-phase critical flow rate at the break points mainly due to the inaccuracies of the critical flow model as well as the quality prediction model. In this study, the critical flow model is improved as a first step that is based on a new sound speed criterion derived from the hyperbolic two-fluid model for non-equilibrium flow and this model is applied to a system analysis code. Following to a conceptual problem of the vertically upward flow with quality variation, the small bottom break of a pressurized horizontal pipe is simulated and discussed in some detail. From the test results without any adjustment like empirical discharge coefficient, the assessment results on the critical flow test through a small bottom break in a horizontal pipe show that just improving the critical flow model can remarkably reduce the relative error.

1. Introduction

Safety significance of a critical flow analysis have led to a development of various empirical and mechanistic critical flow models for the analysis code of pressurized vessels or power plants, such as Moody [1], Henry and Fauske [2], Trapp and Ransom [3] models, and so on. However, the accuracy of these models is still in question especially on the non-equilibrium critical flow conditions.

MARS code [4] is a multidimensional Thermal Hydraulic (T/H) system code developed by Korea Atomic Energy Research Institute (KAERI) for realistic Loss-Of-Coolant Accident (LOCA) simulations of light water reactor transients under the nuclear R&D program of the government. The first version of MARS code was developed by unifying RELAP5/MOD3 [5] and COBRA-TF [6] in the form of one-dimensional (1D) and three-dimensional (3D) modules of the codes. In addition, for a multi-purpose coupled safety analysis, the MARS was coupled with 3D core kinetics code, MASTER, and containment analysis code, CONTEMPT4/MOD5. This enables more realistic analyses for thermal hydraulics of multidimensional system, where strong feedbacks from core kinetics and containment response are taken care of.

E-mail address: s_clarinet@hotmail.com

0022-460X/$ - see front matter
doi:10.1016/j.jsv.2008.01.049

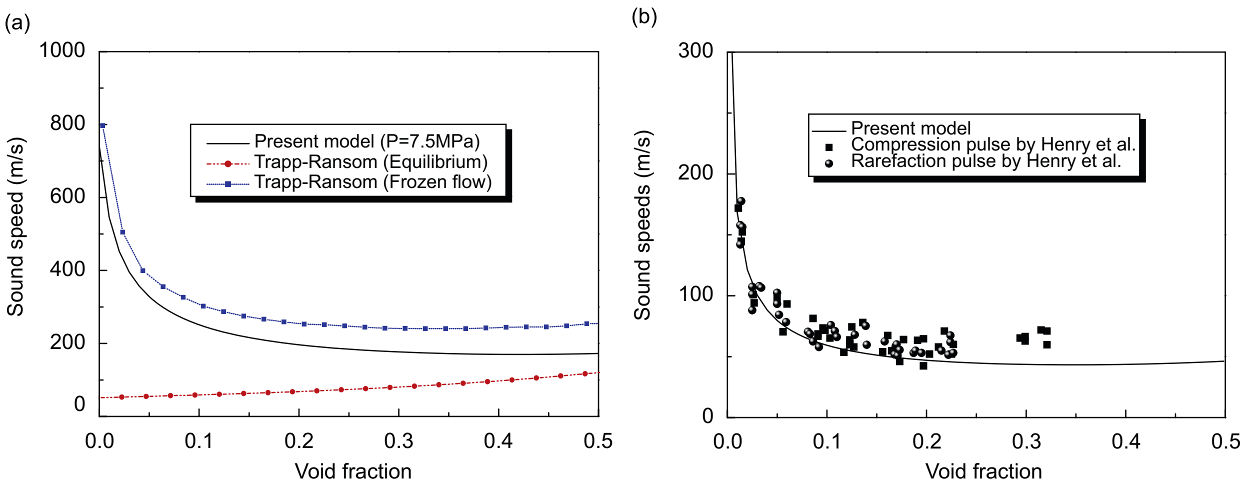

Fig. 1. (a) Present sound speed vs. Trapp & Ransom's model and (b) sound speed criterion ($p = 283$ kPa).

MARS code accounts for the phase separation phenomena and computes the flux of mass and energy through the off-take attached to the bottom of a horizontal pipe when stratified conditions occur in the horizontal pipe. The importance of predicting the flow conditions through an off-take in a Small Break LOCA has been discussed. However, the predicted flow conditions like sound speed and quality at the break point also have difficulties as will be mentioned in Section 5. Furthermore, one of the important assumptions used for MARS code [4] is that the fluid within a given control volume is homogeneously mixed. The homogeneously mixed assumption ignores such phase separation and causes additional computational errors.

In this study, as a fist step, a new critical flow model derived analytically from the characteristic analysis of hyperbolic two-fluid equations for two-phase flow is applied to the MARS code [4] in order to simulate the critical mass flow discharge. The original critical flow model of the MARS code [4] has been based on the Trapp & Ransom model [3]. The model incorporated an analytic critical flow model for non-homogeneous, equilibrium two-phase flow consisting of overall mass conservation, two momentum equations and the mixture entropy equation. The momentum equations include interface force terms, called virtual mass terms [7–9], representing the relative acceleration of a bubble in the liquid. They finally derived an analytic critical flow model that contains both relative phasic acceleration terms and derivative-dependent mass transfer terms using the characteristic analysis [3,5].

However, it is well known that the Trapp & Ransom model seriously under-predicts the sound speed on the bubbly flow regime, $\alpha_g < 0.5$, with a discontinuity when approaching the single-phase water condition, $\alpha_g \to 0$, as shown in Fig. 1(a). Because one of the important features of the equilibrium model is the discontinuity in fluid properties that occurs at the saturation line, there is a discontinuous variation of the sound speed at a transition point using the Trapp & Ransom model [3]. However, the earlier experimental data for various conditions do not show such a non-physical discontinuity as shown in Fig. 1(b).

On the other hand, the Trapp & Ransom model can be derived from the frozen flow assumption excluding phase change, which over-predicts the sound speed in the bubbly flow regime so that the critical flow rate can be over-estimated. Therefore, sound speed criteria under the equilibrium and the frozen flow assumptions show good thermodynamic boundaries of lower and upper limits in the two-phase flow, respectively. As a result, it is reasonable that the sound speed of non-equilibrium two-phase flow should exist between these boundaries as shown in Fig. 1(a).

2. Critical flow model

The present author and the previous coworkers had proposed the improved sound speed criteria for bubbly, slug, and annular flow regimes [9,10]. They had introduced new terms, namely, interfacial pressure jump terms based on the surface tension effect in the momentum equations. Although they are relatively very small, compared with the other terms of the momentum equations, they can make the equation system hyperbolic even without conventional virtual mass or artificial viscosity terms.

Referring to the previous study [10] briefly, the hyperbolic 1D two-fluid, six-equation model can be written as follows:

Mass equations,

$$\frac{\partial(\alpha_k \rho_k)}{\partial t} + \frac{\partial(\alpha_k \rho_k v_k)}{\partial x} = 0. \tag{1}$$

Momentum equations,

$$\frac{\partial(\alpha_k \rho_k v_k)}{\partial t} + \frac{\partial(\alpha_k \rho_k v_k^2)}{\partial x} + \alpha_k \frac{\partial p_k}{\partial x} + (p_k - p_i)\frac{\partial \alpha_k}{\partial x} = 0. \tag{2}$$

Energy equations,

$$\frac{\partial(\alpha_k \rho_k u_k)}{\partial t} + \frac{\partial(\alpha_k \rho_k v_k u_k)}{\partial x} + p_k \frac{\partial \alpha_k}{\partial t} + p_k \frac{\partial(\alpha_k v_k)}{\partial x} = 0, \tag{3}$$

where α_k, ρ_k, p_k, v_k, and u_k are volume fraction, density, pressure, velocity, and internal energy, respectively. The subscript $k = g$ is for gas and $k = 1$ is for liquid. We use density and internal energy by function of pressure and temperature for thermal non-equilibrium condition. On the contrary, Trapp & Ransom's model [3] derived from the assumption of thermal equilibrium by using the density and entropy for each phase as a function of pressure only.

The interfacial pressure jump terms, Chung et al. [9] derived the last term on the left-hand side of Eq. (2), as the following form based on the Young & Laplace equation:

$$(p_g - p_i)\frac{\partial \alpha_g}{\partial x} = L_m\left(1 - \frac{R_g}{2}\frac{\partial a_i}{\partial \alpha_g}\right)\frac{\partial \alpha_g}{\partial x} = C_i L_m \frac{\partial \alpha_g}{\partial x}, \tag{4}$$

$$(p_l - p_i)\frac{\partial \alpha_l}{\partial x} = -L_m\left(1 + \frac{R_l}{2}\frac{\partial a_i}{\partial \alpha_l}\right)\frac{\partial \alpha_l}{\partial x} = -C_i L_m \frac{\partial \alpha_l}{\partial x}, \tag{5}$$

where L_m is the bulk modulus of two-phase mixture. We can use the interfacial area density relation, $a_1 = 3.6\alpha_g/D_{\rm ave}$ for the bubbly flow. The averaged bubble diameter $D_{\rm ave}$ is generally obtained by using the Weber number definition, ${\rm We} \equiv 2D_{\rm ave}\rho_l(v_g - v_l)^2/\sigma$. However, if we assume that bubble inner radius R_g and bubble outer radius R_l between the surface thickness are equal to one-half of the averaged bubble diameter $D_{\rm ave}$ then the coefficient of interfacial pressure jump C_i becomes constant with an order of magnitude $O(10^{-1})$.

For the bubbly flow as homogeneous mixture, we can write the fluid bulk modulus with volume fraction definition $\alpha_k = V_k/V$ (V: total volume of a pipe section, V_k: k-phase volume in that section) as

$$L_m = -V\frac{{\rm d}p}{{\rm d}V} = -V\frac{{\rm d}p}{{\rm d}V_g + {\rm d}V_l} = V\frac{{\rm d}p}{V_g\,{\rm d}p/L_g + V_l\,{\rm d}p/L_l}. \tag{6}$$

Since the fluid bulk modulus for each phase is $L_k \equiv \rho_k c_k^2$ and it holds that $L_g \ll L_l$, the fluid bulk modulus multiplied by the coefficient of interfacial pressure jump yields

$$C_i L_m \approx C_i L_g/\alpha_g, \tag{7}$$

which is true in the range $\alpha_g \geqslant L_g/L_l$. We also assume here that the order of magnitude of the mixture bulk modulus multiplied by the constant C_i is almost equal to that of the gas by taking $\alpha_g \approx O(10^{-1})$ for bubbly flow, and then it gives $C_i L_m = \rho_g c_g^2$. Here c_g is the sound speed for gas. Therefore, we finally obtain

$$(p_k - p_i)\frac{\partial \alpha_k}{\partial x} = (-1)^n L_m \frac{\partial \alpha_k}{\partial x}, \tag{8}$$

where the exponent n stands for the liquid if $n = 1$ and for the gas if $n = 2$.

Using a thermodynamic isentropic relation $(\partial \rho_k/\partial p_k)_{s_k} = 1/c_k^2$ and the equality $\partial p_g/\partial x = \partial p_l/\partial x$ from the derivatives on the Young and Laplace equation, the eigenvalues of the above equation system can be obtained analytically as the roots of a sixth-order polynomial equation: To obtain the eigenvalues of the governing

Table 1
System eigenvalues

Flow regime	Eigenvalues
Bubbly flow	$\lambda_{1,2} = v_g, v_1$ $\lambda_{3,4} = v_g \pm c_g$ $\lambda_{5,6} = v_l \pm c_l\sqrt{\rho_g c_g^2/\alpha_l \rho_g c_g^2 + \alpha_g \rho_l c_l^2}$

equation system, we changed the mathematical form of Eqs. (1)–(3) into a matrix form. Then the non-homogeneous, non-equilibrium governing equations become

$$\frac{\partial U}{\partial t} + G\frac{\partial U}{\partial x} = E, \tag{9}$$

where $U = [\alpha_g \quad p_g \quad v_g \quad v_l \quad u_g \quad u_l]^{\mathrm{T}}$ is a primitive variable vector. The eigenvalues of coefficient matrix G in Eq. (9) are determined by obtaining six roots of the following sixth-order polynomial equation:

$$P_6(\lambda) = (\lambda - v_g)(\lambda - v_l)\left[K_1\lambda^4 + K_2\lambda^3 + K_3\lambda^2 + K_4\lambda + K_5\right] = 0, \tag{10}$$

where the coefficients, $K_{1,\ldots,5}$, are

$$K_1 = 1, \quad K_2 = -2(v_g + v_l),$$
$$K_3 = (v_g + v_l)^2 + 2v_g v_l - (c_g^2 + c_l^2),$$
$$K_4 = 2\{v_g(c_l^2 - v_l^2) + v_l(c_g^2 - v_g^2)\},$$

and

$$K_5 = (c_l^2 - v_l^2)(c_g^2 - v_g^2).$$

According to the closed-form solution of Eq. (10), system eigenvalues consist of two convective velocities and the conjugates of sound speeds for the gas and the liquid phases as listed in Table 1. Two of them, λ_3 and λ_5, with zero phasic velocities ($v_g = v_1 = 0$) represent the sound speeds of the gas and the liquid phase, respectively.

Therefore, the total sound speed C of the non-equilibrium bubbly flow has the volume fraction weighting of the eigenvalues as

$$C = \frac{\lambda_3\lambda_5}{\alpha_l\lambda_3 + \alpha_g\lambda_5} = \frac{c_g c_l\sqrt{\rho_g c_g^2/\alpha_l\rho_g c_g^2 + \alpha_g\rho_l c_l^2}}{\alpha_l c_g + \alpha_g c_l\sqrt{\rho_g c_g^2/\alpha_l\rho_g c_g^2 + \alpha_g\rho_l c_l^2}}, \tag{11}$$

where c_k is the sound wave propagation speed of phase k.

For bubbly flow with vapor and liquid, the predicted sound speed (11) agrees well with the experimental data [11] of the void fraction range, $0 < \alpha_g \leqslant 0.3$, as shown in Fig. 1(b). If there was no vapor, $\alpha_g \to 0$, the predicted sound speed of two-phase fluid becomes that of single-phase water, $\lim_{\alpha_g \to 0} C = C_l$.

3. Critical flow test procedure

One subroutine contains the critical flow model for two-phase flow, which is used as a boundary condition to obtain flow solutions in the MARS code [4]. We impose the implemented critical flow model on the junction test to determine whether the flow is critical or not. When the critical flow occurs, the fluid velocity equals to the sound speed prohibiting the signals from propagating to the upstream. Then Eq. (12) is brought up-to-date in terms of new-time phasic velocities and it is solved in conjunction with a difference momentum equation (13):

$$\frac{\alpha_g \rho_g v_g + \alpha_l \rho_l v_l}{\alpha_g \rho_g + \alpha_l \rho_l} = C, \tag{12}$$

$$\rho_g \left(\frac{\partial v_g}{\partial t} + \frac{1}{2} \frac{\partial v_g^2}{\partial x} \right) - \rho_l \left(\frac{\partial v_l}{\partial t} + \frac{1}{2} \frac{\partial v_l^2}{\partial x} \right) = (\rho_g - \rho_l) B_x + \Phi, \tag{13}$$

where B_x is gravitational acceleration. The symbol Φ includes phasic and interfacial friction terms and momentum source terms. Therefore, the phase slip is not permitted. It should also be noted that the present model differs from the Trapp & Ransom model in defining the Mach number criterion (12): Namely, the Trapp & Ransom Mach number criterion was derived as follows:

$$\frac{\alpha_g \rho_l v_g + \alpha_l \rho_g v_l}{\alpha_g \rho_l + \alpha_l \rho_g} \equiv C_{\mathrm{he}}. \tag{14}$$

As mentioned before, we do not use the sound speed C_{he} in the right-hand side of Eq. (14) on the homogeneous equilibrium condition anymore.

In addition, we now use the two-phase mixture velocity

$$v \equiv \frac{\alpha_g \rho_g v_g + \alpha_l \rho_l v_l}{\alpha_g \rho_g + \alpha_l \rho_l}, \tag{15}$$

which is derived by the mass conservation of two-phase fluid, instead of the Trapp & Ransom mixture velocity, namely, the left-hand side of Eq. (14). Because the Trapp & Ransom mixture velocity was highly simplified to obtain an analytic form, the velocity does not satisfy the mass conservation of two-phase fluid. For that reason, this velocity can be treated as a pseudo-velocity of the two-phase fluid.

Calculating thermal hydraulic phenomena using the MARS code [4], critical flow is assumed to occur at the Mach number of unity. However, because the plant grid generation for system analysis is generally very coarse, we assume that the critical flow occurs at the grid point where the Mach number is greater than, or equal to 1:

$$M \equiv \frac{v}{C} \geqslant \pm 1. \tag{16}$$

4. Critical flow with quality variation

The Trapp & Ransom model has one more behavior that is non-physical during the quality variation. That is to say, the variation of quality from the single-phase water to two-phase fluid under the critical flow condition is not smooth. To compare the trends of quality and mass flow rate especially in the quality range of $0<x<0.1$, we consider a following conceptual problem on the critical flow with quality variation.

The vertical flow through 1 m-length pipe with constant pressure difference, $p_i - p_o = 0.4\,\mathrm{MPa}$, between the inlet and the outlet is assumed to calculate critical flow with inlet quality variation as shown in Fig. 2. Owing to the sufficient pressure difference, the vertical upward flow is always a critical flow. However, the quality increase from the pipe inlet makes the critical flow rate decreased.

At the initial stage, the vertical upward flow of single-phase water is maintained until 10 s. Then the single-phase flow is a critical flow, and the mass flow rates are kept constant at the pipe outlet as shown in Fig. 3(a). However, the initiation of quality increases from $x = 0$ to 0.1 reduces the mass flow rates. At the same time, the results using the present model show that the quality increase causes a small undershoot before the monotonic decrease of mass flow rate. On the contrary, the Trapp & Ransom model shows a cutting of mass flow rate, before monotonic decrease.

In addition, it should also be noted that the mass flow rate calculated by the Trapp & Ransom model is smaller than the present model. Because the calculated mass flow rate is in proportion to the predicted sound

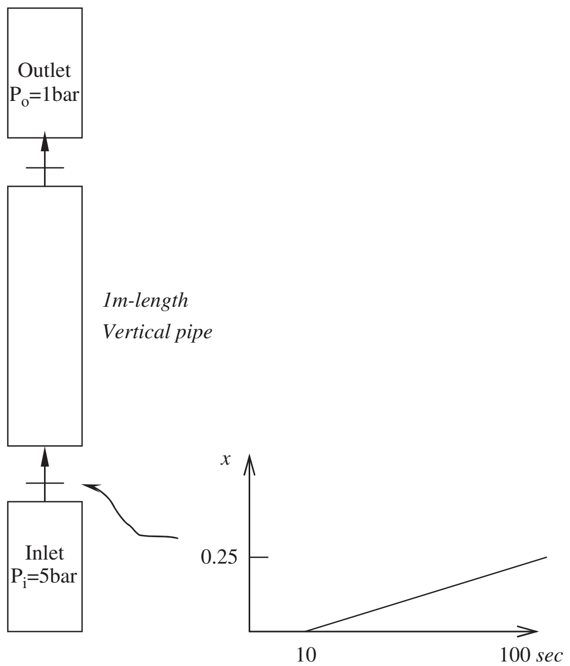

Fig. 2. Vertically upward critical flow with quality variation.

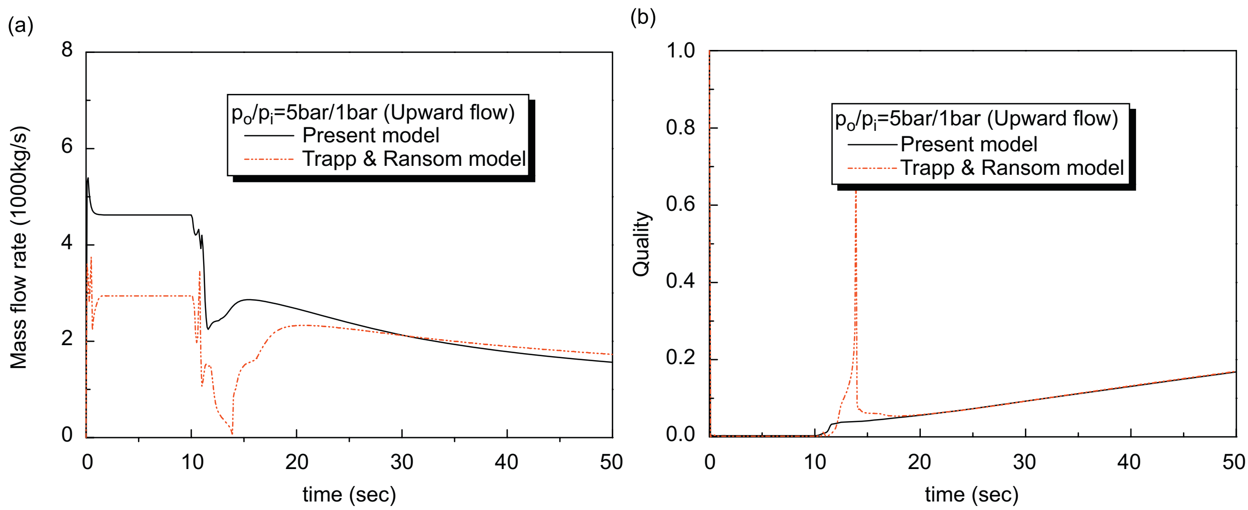

Fig. 3. (a) History of mass flow rate on the vertically upward critical flow and (b) quality variation on the vertically upward critical flow.

speed, the calculated mass flow rates of this conceptual problem are compatible with the results shown in Fig. 1(a).

The quality variation at the pipe outlet in Fig. 3(b) also shows the difference on the characteristic of the Trapp & Ransom model compared with the present model. Owing to the dubious peak of quality at about 13 s, the mass flow rate becomes the minimum at this time. Consequently, it is confirmed that the present model improves the trend of quality variation as well as that of the critical flow rate.

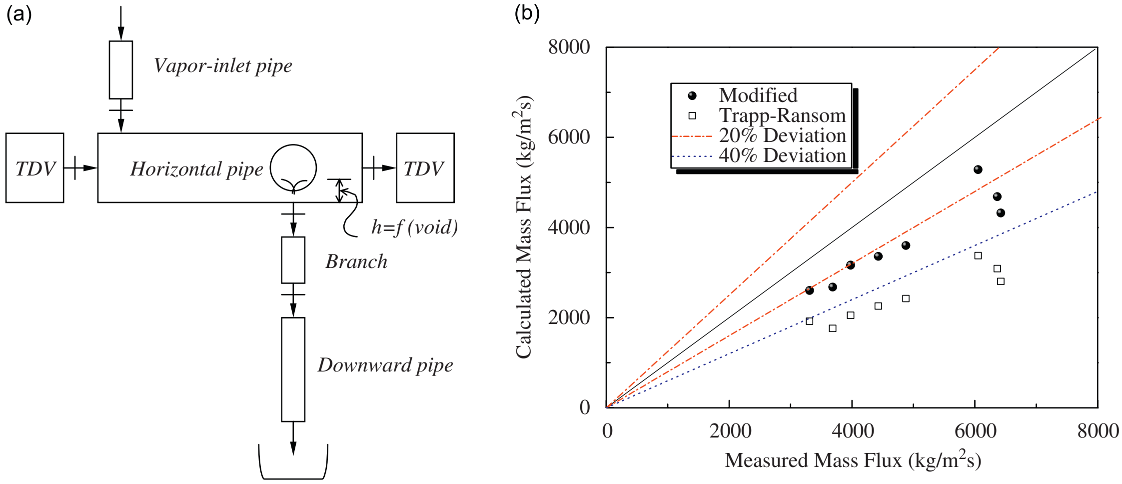

Fig. 4. (a) Small bottom break of a horizontal pipe (HSVPM tests nodalization) and (b) calculated results vs. experimental data for HSVPM tests.

5. Small bottom break of a horizontal pipe

The second example deals with an important critical flow problem produced by the small bottom break in a pressurized horizontal pipe. In this case, downward water discharge mechanism can be interrupted by the onset of the vapor pull-through as shown in Fig. 4(a). However, as pointed out in Ref. [4], an interruption on the discharged water cannot be predicted exactly because the quality prediction model as if Horizontal Stratification Vapor Pull-through Model (HSVPM) is inaccurate at the bottom break during the vortex accompanied vapor pull-through occurs.

In this case, water will flow through the bottom break until the water level start to approach (but not reach) the bottom of the pipe, at which time some vapor will be pulled through the water layer and the fluid quality at the break will increase. For these reasons, the critical flow rate through the off-take branch connected with the bottom break is decreased by the vapor pull-through in comparison with the case without this phenomenon.

The MARS code [4] using the horizontal stratification vapor pull-through model that based on that of the RELAP5/MOD3 code [5] accounts for the phase separation phenomena and computes the flux of mass and energy when stratified conditions occur in the horizontal pipe. Zuber [12] has discussed the importance of predicting the fluid conditions through a small bottom break in some detail. There are several experiments of the phenomena that are relevant to small break flows for vapor-water fluids.

Using the earlier experimental data, we can show that in most cases the height or water level for the onset of vapor pull-through can be defined as follows [13]:

$$h_o = \frac{\mathrm{CW}_k^{0.4}}{[g\rho_l(\rho_l - \rho_g)]^{0.2}}, \tag{17}$$

where the value of C for the onset of vapor pull-through in a bottom breaks is greatly influenced by the water flow rate in the main pipe. A value of 1.5 is used to characterize the experimental data for the onset of vapor pull-through. The variable W_k is the mass flow rate of continuous phase in the off-take. In addition, the flow quality through a bottom break can be derived as follows:

$$x = x_o^{2.5R}\left[1 - 0.5R(1 + R)x_o^{1-R}\right]^{0.5}, \tag{18}$$

where $R = h/h_o$ and $x_o = 1.15/1 + (\rho_l/\rho_g)^{0.5}$.

Calculating the vapor quality at the break using Eq. (18), errors can exists between the test results and the experimental data at the entrance of the bottom break in a horizontal pipe mainly due to the inaccuracy of

Table 2
Test matrix for HSVPM

No.	h (mm)	p (kPa)	T_o	j_l (kg/s)	j_g (kg/s)	Q_{exp} (kg/m^2 s)
1	16.5	367	140.7	0.0096	0.0403	3698
2	13.5	445	147.9	0.0082	0.0537	3322
3	14.8	506	151.9	0.0087	0.0784	3992
4	14.0	575	157.8	0.0103	0.0602	4441
5	14.2	625	160.6	0.0149	0.0878	4891
6	17.5	760	168.2	0.0136	0.0626	6435
7	18.1	860	174.0	0.0135	0.0379	6378
8	18.3	980	179.0	0.0192	0.0918	6067

water level (R) prediction. Actually, due to the inaccuracy of quality prediction model as well as that of the critical flow model, the calculated critical flow rates also show up to 50% underestimation comparing with the experimental data as plotted in Fig. 4(b). Nevertheless, it should be noted that we try to reduce not the inaccuracy of HSVPM but that of the critical flow model adopted in the MARS code in this study. Fortunately, a great part of each discrepancy especially due to the inaccuracy of the critical flow model can be reduced by improving the critical flow model.

To calculate critical flow rate, the flow pattern at the break point on the bottom of a horizontal pipe can be assumed as bubbly flow. Eight tests on different heights h(m) of surface under the various conditions of pressure p(kPa) are listed in Table 2 and they are calculated to compare the results of the present critical flow model with those of the Trapp & Ransom model. In this study, we keep the heights h(m) of flowing water in the upstream of the bottom break constant.

The results plotted in Fig. 4(b) show that the present model could reduce the relative errors obtained from the Trapp & Ransom model: The relative errors of the present model are reduced to about 25%, which are much smaller than those obtained from the Trapp & Ransom model. Therefore, it can be concluded that the critical flow model as well as HSVPM has to be improved in order to calculate the critical flow through the bottom break in a horizontal pipe more accurately.

6. Concluding remarks

Derived from the hyperbolic two-fluid equations for the non-equilibrium, non-homogenous flow, a newly improved critical flow model for two-phase flow is implemented into the system analysis code. Eigenvalues of the two-fluid equations show reasonable trends of the sound speeds compared with the experimental data.

Treating the vertical upward flow with quality variation, the present model improves the trends of mass flow rate and quality variation by reducing the dubious peaks relevant to the flow regime transition from single-phase water to two-phase fluid. In addition, calculated results of the critical flow at the small bottom break in a pressurized horizontal pipe show that improving the critical flow model even though there is no modification of the quality prediction model can remarkably reduce the relative errors. Therefore, the critical flow model as well as the quality prediction model (HSVPM) should be improved to increase the accuracy of the critical flow rate through the bottom break in the horizontal pipe.

Acknowledgments

This research was performed for the Hydrogen Energy R&D Center, one of the 21st Century Frontier R&D Programs, funded by the Ministry of Science and Technology of Korea and the author would like to acknowledge the valuable contributions of Dr. Won-Jae Lee in Korea Atomic Energy Research Institute.

References

[1] F.J. Moody, Maximum flow rate of a single-component, two-phase mixture, *Transactions of ASME, Journal of Heat Transfer* 87 (1965) 134–142.

[2] R.E. Henry, H.K. Fauske, The two-phase critical flow of one-component mixtures in nozzles, orifices, and short tubes, *Transactions of ASME, Journal of Heat Transfer* 93 (1971) 179–187.

[3] J.A. Trapp, V.H. Ransom, Choked flow calculation criterion for nonhomogeneous, nonequilbrium two-phase flows, *International Journal of Multiphase Flow* 8 (1982) 669–681.

[4] W.J. Lee, Development of a multi-dimensional thermal hydraulic system code, MARS 1.3.1, *Annals of Nuclear Energy* 25 (1999) 1611–1642.

[5] RELAP5/MOD3.2.2 Code Manual, Vol. IV: Models and Correlations, EG&G Idaho, Inc., NUREG/CR-5535, 1998.

[6] M. J. Thurgood, COBRA/TRAC—a thermal-hydraulics code for transient analysis of nuclear reactor vessels and primary coolant systems, NUREB/CR-3046, PNL-4385, 1983.

[7] D.A. Drew, L.Y. Cheng, R.T. Lahey Jr., The analysis of virtual mass effects in two-phase flow, *International Journal of Multiphase Flow* 5 (1979) 233–242.

[8] A.R.D. Thorley, D.C. Wiggert, The effect of virtual mass on the basic equations for unsteady one-dimensional heterogeneous flows, *International Journal of Multiphase Flow* 12 (1985) 149–160.

[9] M.S. Chung, S.J. Lee, K.S. Chang, Effect of interfacial pressure jump and virtual mass terms on sound wave propagation in the two-phase flow, *Journal of Sound and Vibration* 244 (2001) 717–728.

[10] M.S. Chung, K.S. Chang, S.J. Lee, Numerical solution of hyperbolic two-fluid two-phase flow model with non-reflecting boundary conditions, *International Journal of Engineering Science* 40 (2002) 789–803.

[11] R.E. Henry, M.A. Grolmes, H.K. Fauske, Pressure pulse propagation in two-phase one- and two-component mixtures, ANL-7792, 1971.

[12] N. Zuber, Problems in modeling of small break LOCA, NUREG-0724, 1980.

[13] B.T. Lubin, G.S. Springer, The formation of a dip on the surface of a liquid draining form a tank, *Journal of Fluid Mechanics* 29 (1967) 385–390.